Supporting Information

Enhanced Radiotherapy using Bismuth Sulfide Nanoagents Combined with Photo-thermal Treatment

Xiaju Cheng[1†], Yuan Yong[3,4†], Yiheng Dai[2], Xin Song[1], Gang Yang[1], Yue Pan[2]*, Cuicui Ge[1]*

1. School of Radiation Medicine and Protection, School for Radiological and Interdisciplinary Sciences (RAD-X), Collaborative Innovation Center of Radiation Medicine of Jiangsu Higher Education Institutions, Soochow University, Suzhou 215123, China

2. State and Local Joint Engineering Laboratory for Novel Functional Polymeric Materials, College of Chemistry, Chemical Engineering and Materials Science, Soochow University, Suzhou 215123, China

3. College of Chemistry and Environment Protection Engineering, Southwest Minzu University, Chengdu 610041, China

4. CAS Key Laboratory for Biomedical Effects of Nanomaterials and Nanosafety, Institute of High Energy Physics, Chinese Academy of Sciences, Beijing 100049, China

[†]Equal contribution

*Corresponding authors: ccge@suda.edu.cn, panyue@suda.edu.cn

Experimental Section

Comet assay.

Briefly, 100 μL of 1% normal agarose was layered on the microscope slides, covered with a cover-slip and put at 4 °C for solidification. The cells after different treatments were collected and mixed with equal volume of 1% low melting agarose at 37 °C. 100 μL of mixture were laid on the precoated slide and covered with a cover-slip as before. Once the layer solidified, the cover-slips were gently removed and slides were immersed in prepared cold lysis solution (2.5 mM NaCl, 100 mM Na_2EDTA, 10 mM Tris, to mix 1% Triton X-100, 10% DMSO, 1% N-Lauroyl Sarcosine Sodium before use) for 1 h at 4 °C in dark place. The slides were then transferred into the electrophoresis buffer (pH 13) for 20 min and then electrophoresis was carried out at 20 V, 200 mA for 20 min.

Finally, the slides were washed twice with neutralization buffer (0.4 M Tris, pH 7.5) and stained with 20 μL of 20 μg/mL EB solution for 1 min. Slides gel were washed twice with double-distilled water. Comet images were analyzed on a fluorescent microscope (Olympus, Japan). Comets were analyzed using the public domain PC-image analysis program CASP software. One hundred cells per sample were randomly selected, *i.e.*, 50 cells were from each of the two replicate slides. The percentage of tail DNA and tail moment (TM) served as the indicator.

Animals.

BALB/c mice were obtained from Chang Zhou Cavens Laboratory Animal Technology Co. Ltd. These mice were housed in stainless steel cages under the standard conditions (25±2 °C, 60±10% relative humidity) with a 12 h light/dark cycle. Distilled water and sterilized food for mice were available ad libitum. Animals were acclimated to this environment for 5 days prior to treatment.

Immediately after being euthanized, blood samples were obtained from Orbital sinus in mice. 1 ml of whole blood is drawn into a tube containing an anticoagulant and mixed thoroughly for blood count. The remaining blood samples were placed at 4 °C for 45 min and then centrifuged at 3000 rpm for 5 min at 4 °C. The serum was collected as the pale white yellow colored supernatant, aliquots were assessed for biochemistry. Rabbit monoclonal anti-Bcl-2, anti-Bax, anti-Caspase 3 (diluted 1:1,000, abcam) were used to stain Bcl-2 and Caspase 3, respectively. Tumor tissues were harvested and incubated with antibody and then immune histochemical following the vendor's instructions. The images were taken with a confocal laser microscopy (FV1200, OLYMPUS, Japan).

Table S1. Blood chemistry analysis of mice receiving single intravenous injection of saline (control) or Bi_2S_3 nanorods followed by dissections in 30 days postinjection.

	Control	Bi_2S_3
AST (U/L)	208±26.2	214.7±22.3
ALT (U/L)	27.7±7.2	26.5±4.2
ALB (g/L)	18.5±1.9	18.±1.3
ALP (U/L)	50.5±6.6	49.5±6.9
Cr-S (μmol/L)	7.7±0.9	7.2±1.2
UREA (mmol/L)	6.8±1.1	6.7±0.7

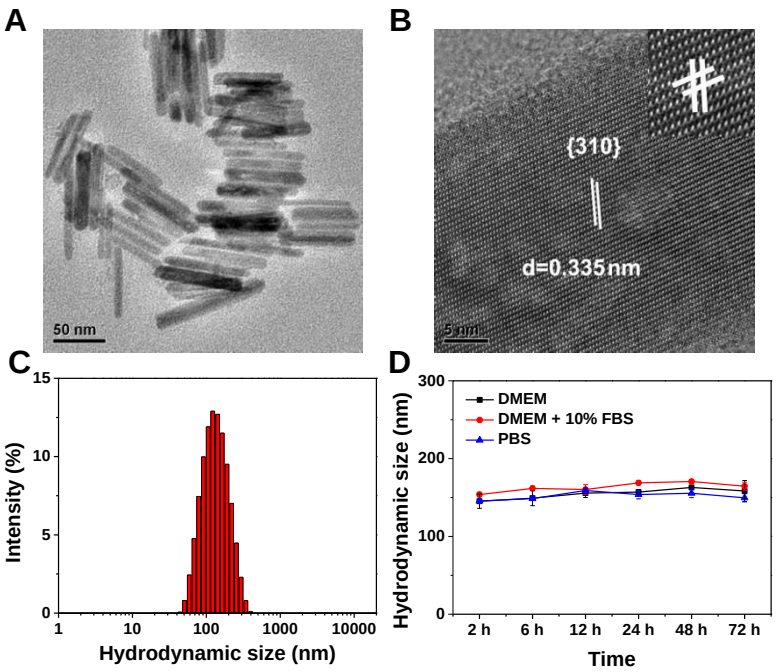

Figure S1. (A,B) HRTEM image of the produced Bi_2S_3 nanorods (C) The hydrodynamic size distribution of Bi_2S_3 nanorods and (D) The hydrodynamic size of Bi_2S_3 nanorods in different media monitored for a 72 h.

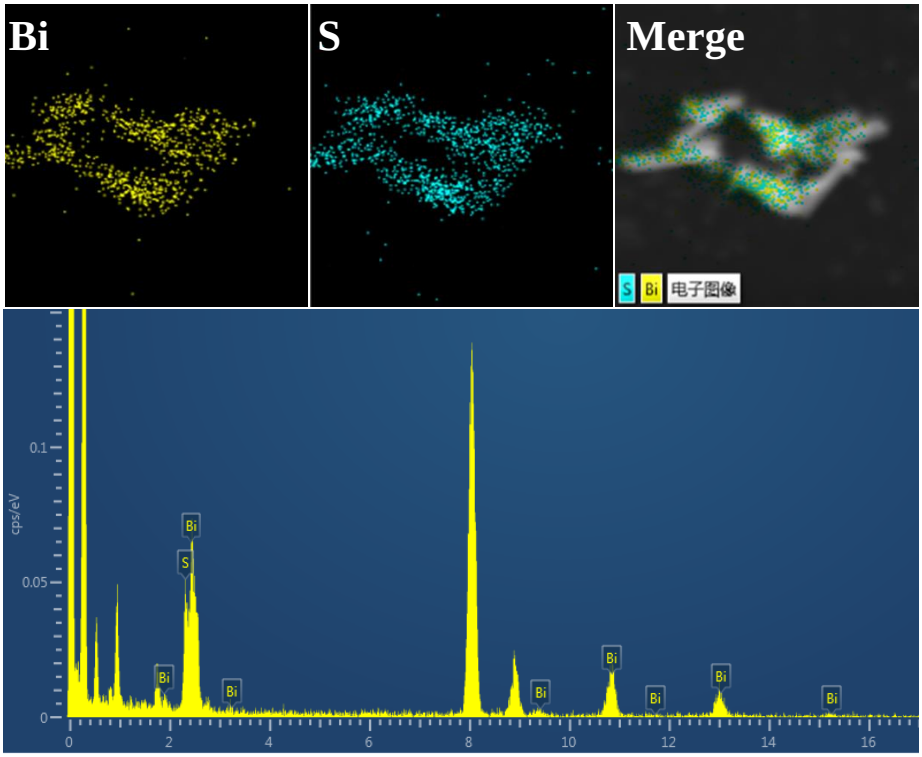

Figure S2. EDS patterns of the produced Bi_2S_3 nanorods.

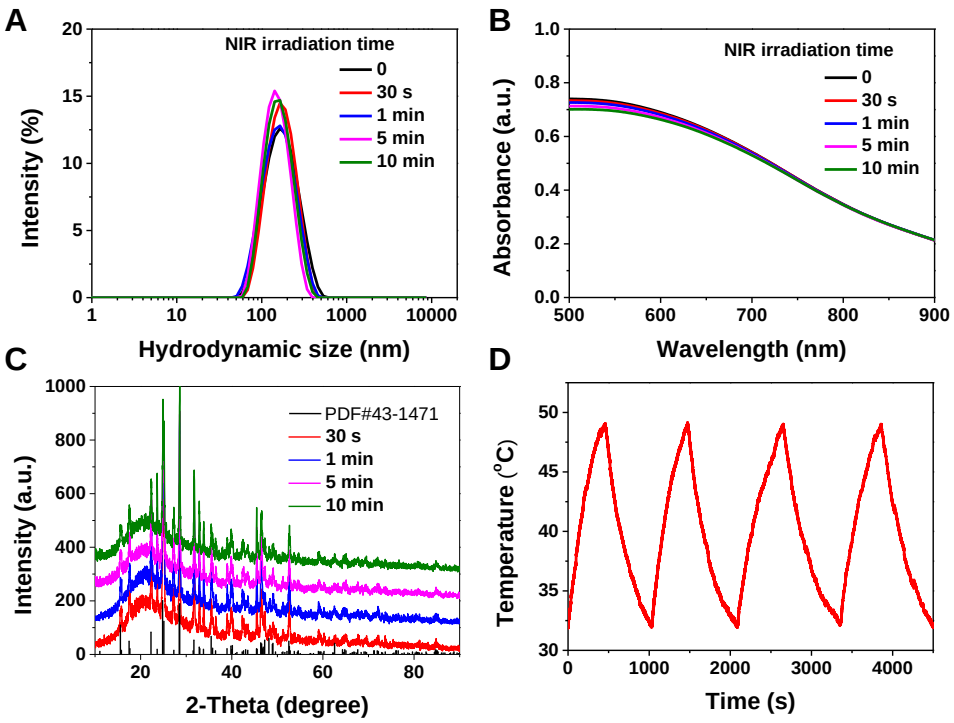

Figure S3. The hydrodynamic size (A), UV-vis absorption spectra (B) and XRD (C) of Bi_2S_3 nanorods upon different NIR irradiation time. (D) The temperature change of Bi_2S_3 nanorods upon different NIR irradiation of 808 nm laser over four laser on/off cycles.

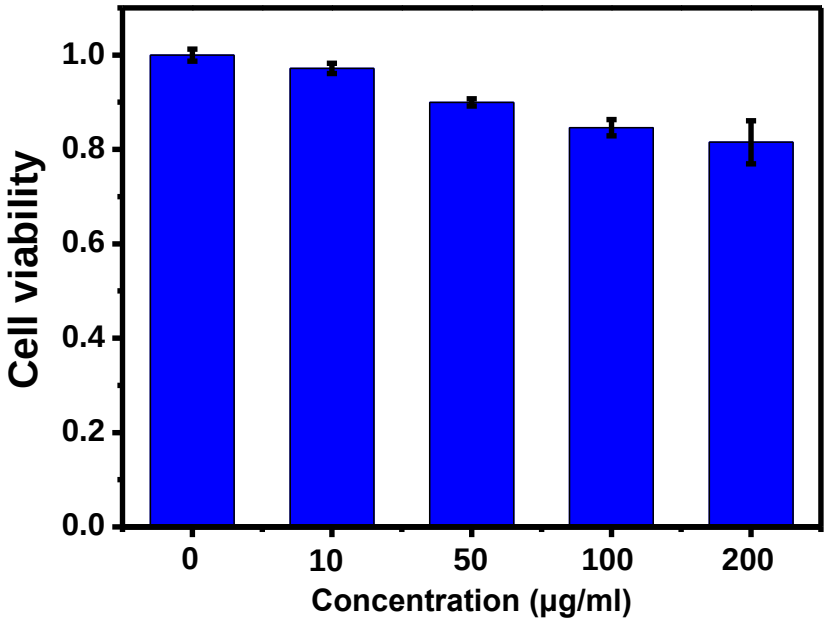

Figure S4. Quantitative analysis of the cell viability with Bi_2S_3 nanorods at varied concentrations using CCK-8. The data are the means and standard deviation from three experiments.

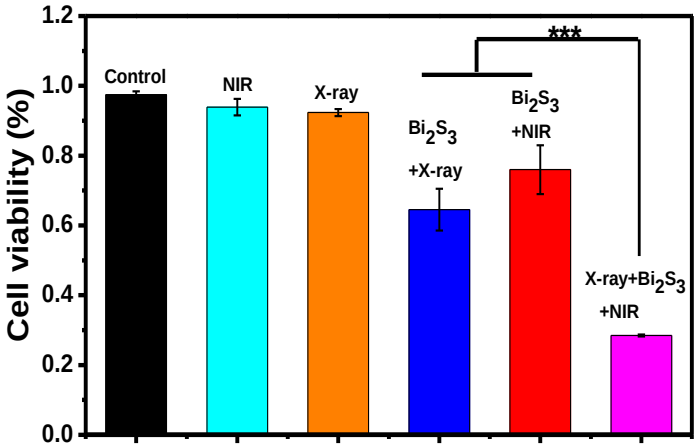

Figure S5. Quantitative analysis of the cell viability of 4T1 cells treated with saline (control), NIR-laser irradiation, X-ray, X-ray + Bi_2S_3 nanorods, Bi_2S_3 + NIR-laser irradiation, and X-ray + Bi_2S_3 + NIR. All NIR-laser irradiation experiments on the cellular level were performed under the same condition (808 nm, 2.0 W/cm^2, 8 min). RT experiments were conducted at the constant dose of 4 Gy (1.23 Gy/min). Error bars represent SD of at least three replicates. p values: ***$p < 0.001$.

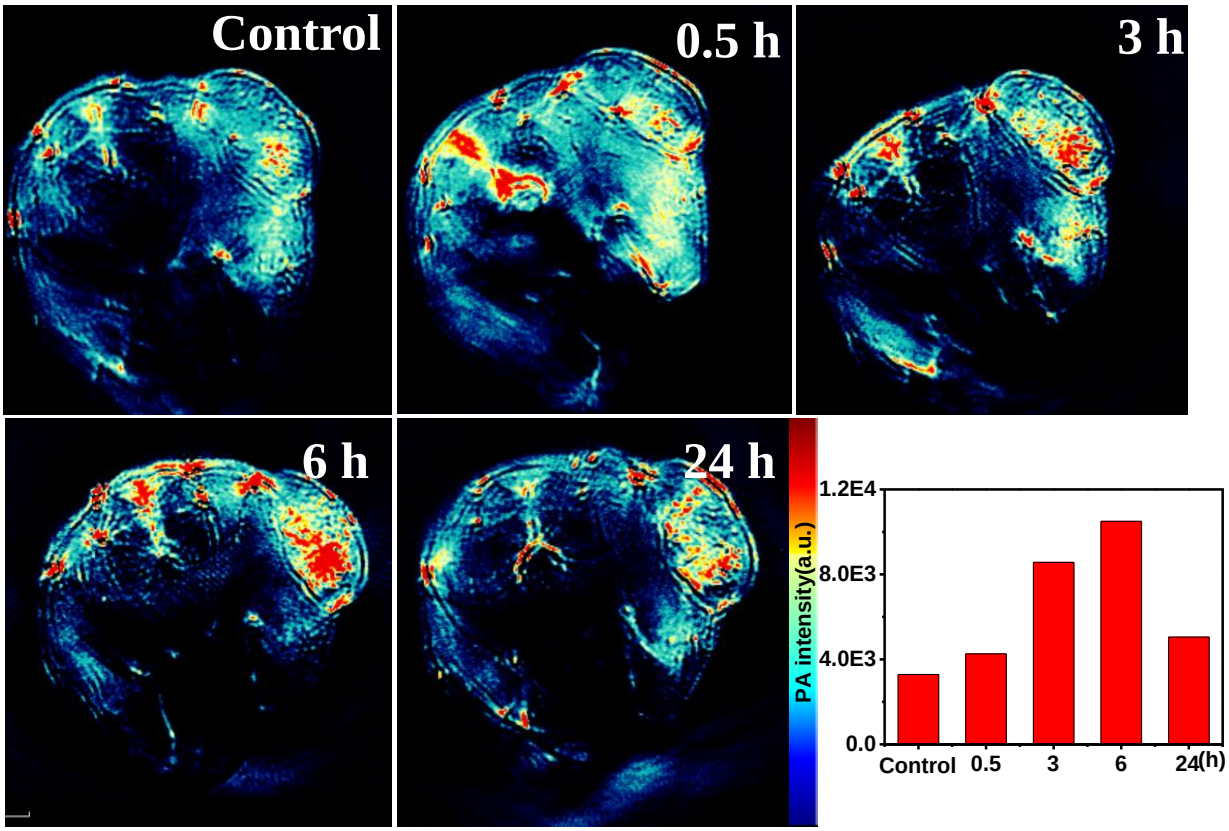

Figure S6. MSOT images of tumor before and after *i.v.* administration of Bi_2S_3 NRs at different time points (0.5, 3, 6, and 24 h).

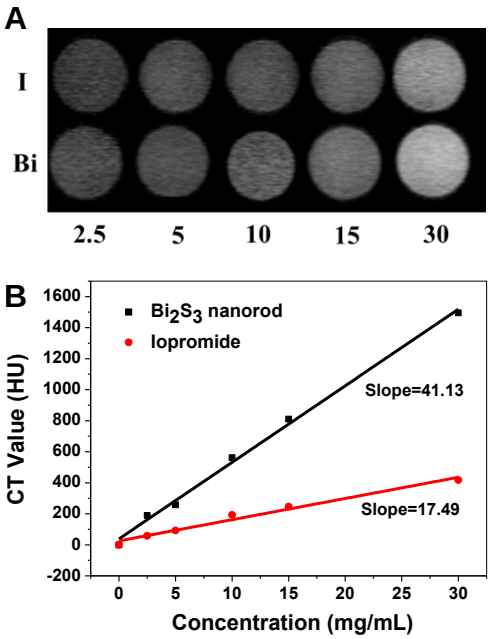

Figure S7. (A) X-ray CT images in vitro of commercially used iopromide and Bi_2S_3 with different concentrations. (B) Hounsfield unit values of iopromide and Bi_2S_3 samples as the function of their corresponding concentrations.

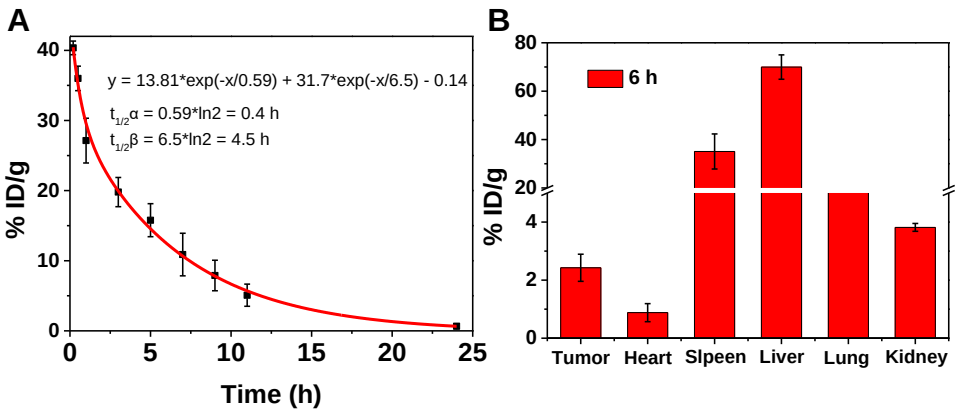

Figure S8. (A) The blood circulation behavior of Bi_2S_3 nanorods. (B) The biodistribution of Bi_2S_3 nanorods at 6 h postejection.

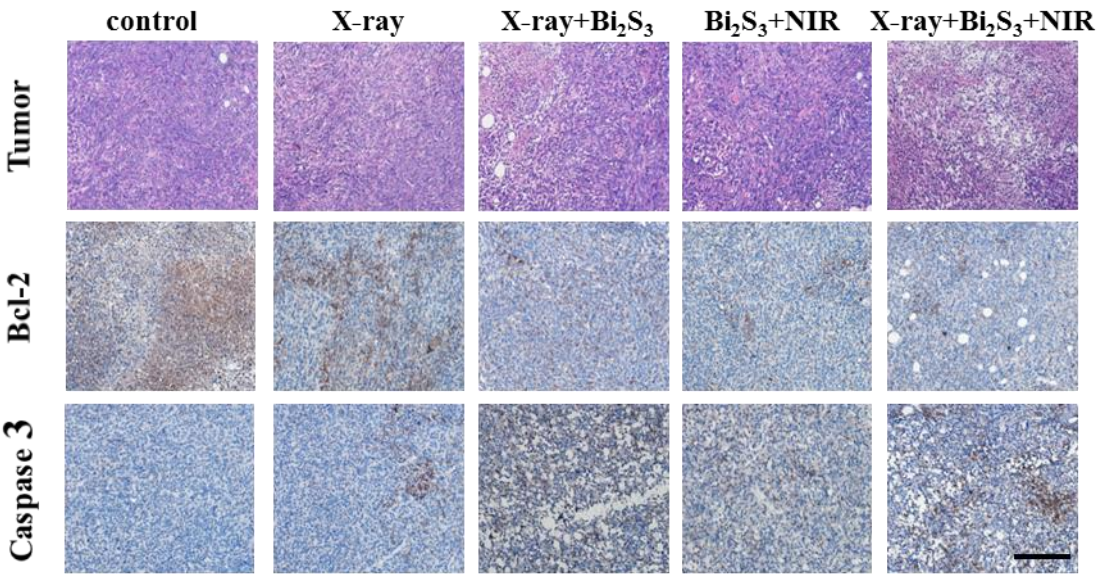

Figure S9. H&E staining and immuno-histochemical analysis for Bcl-2 and Caspase-3 from 4T1 tumors with different treatments. Scale bar corresponds to 100 μm.

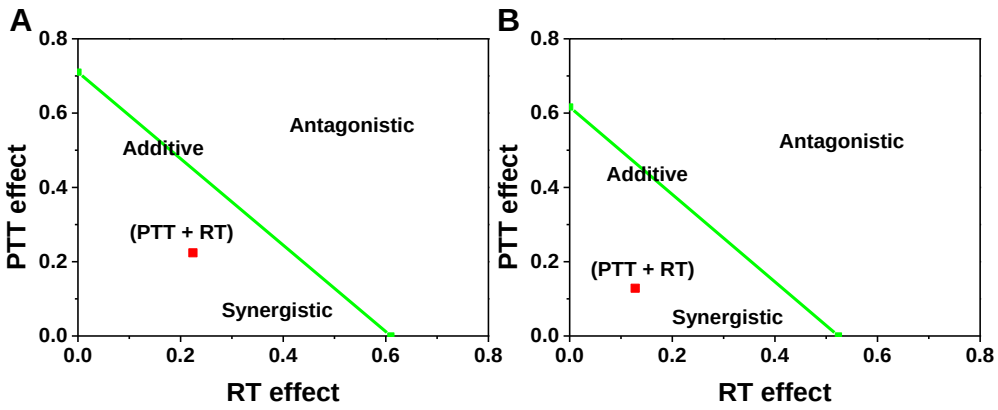

Figure S10. Isobologram analysis of the synergistic anticancer effect of the combined application of photothermal therapy and radiotherapy *in vitro* (A) and *in vivo* (B) assay. The data points in the isobologram correspond to the growth inhibition ratio in the combined treatment.

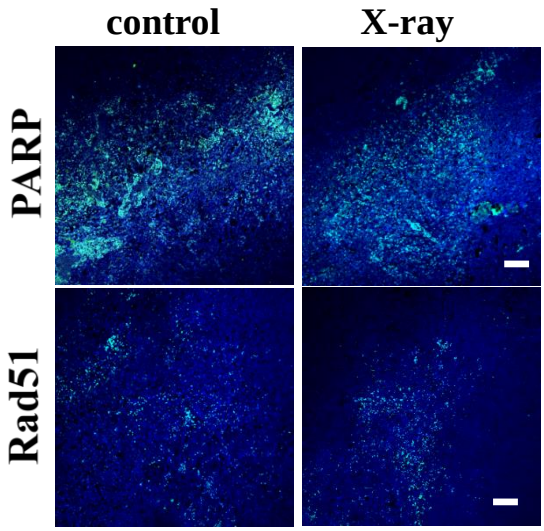

Figure S11. Representative images of immunofluorescent staining of PARP (Upper figures) and rad51 (lower pictures) in continuous sections from 4T1 tumors after treatment with saline/X-ray (positive expression: bright green regions). Scale bar corresponds to 100 μm.

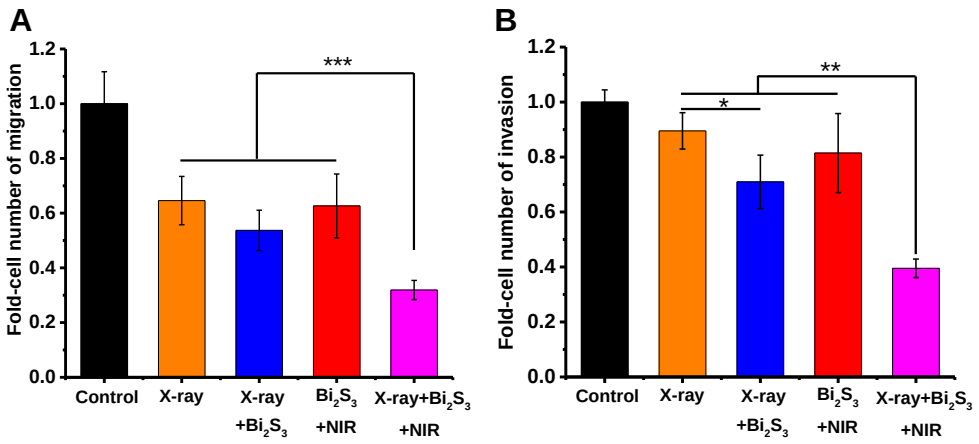

Figure S12. The number of migration cells (A) and invasion cells (B) after different treatments. The data are the means and standard deviation from three experiments. *P* values were calculated by the student's test: **p* < 0.05, ***p* < 0.01, ****p* < 0.001.

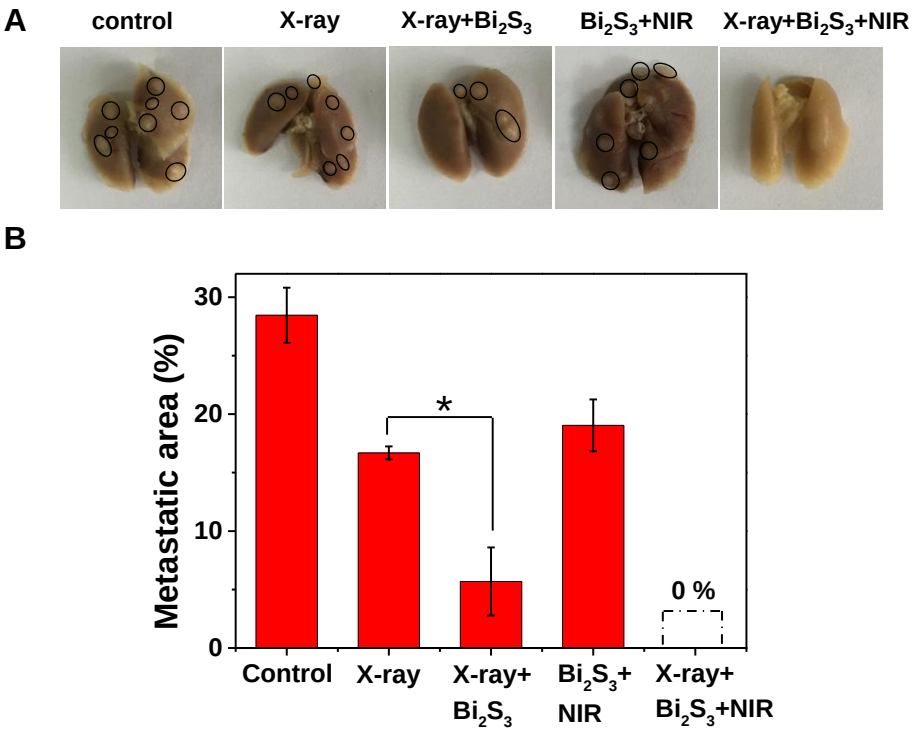

Figure S13. (A) Macroscopic pictures of lungs from five treatment groups. Tumor metastasis sites are highlighted by black circles. (B) Lung metastasis burden was calculated by counting the area of tumor nodules on the lung surface (n=3). Error bars represent standard deviation of the mean. *P* values were calculated by the student's test: $*p < 0.05$.

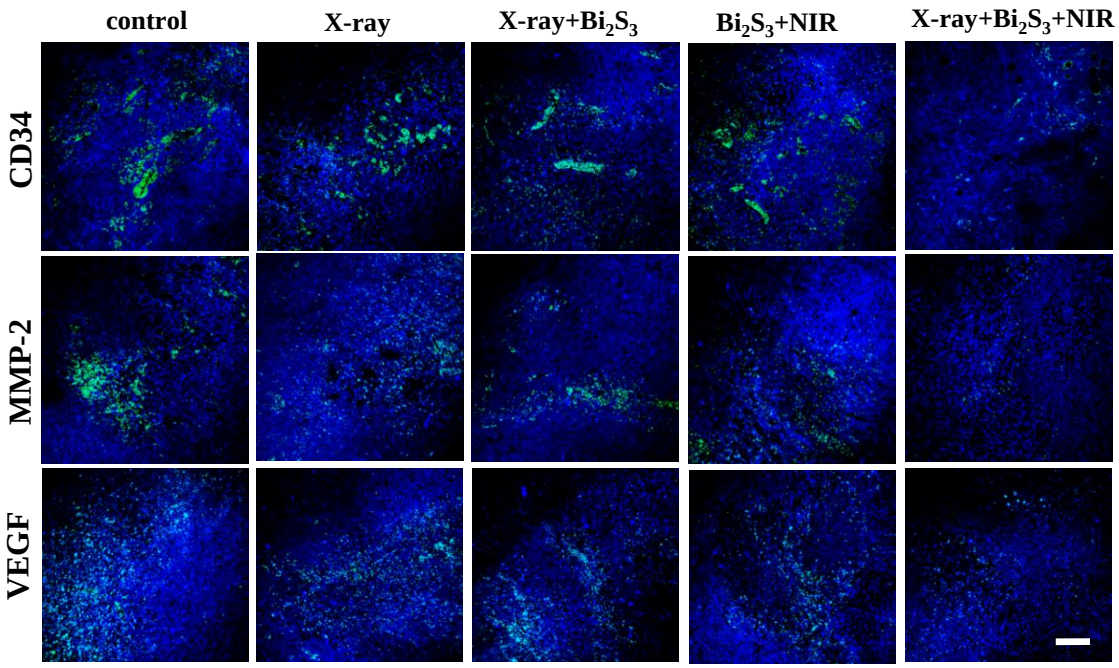

Figure S14. Mechanism of combined cancer treatment on anti-tumor metastasis. Representative immunofluorescent staining for CD34, MMP-2, and VEGF in continuous sections from 4T1 tumors with different treatments (positive expression: bright green regions). Scale bar corresponds to 100 μm.

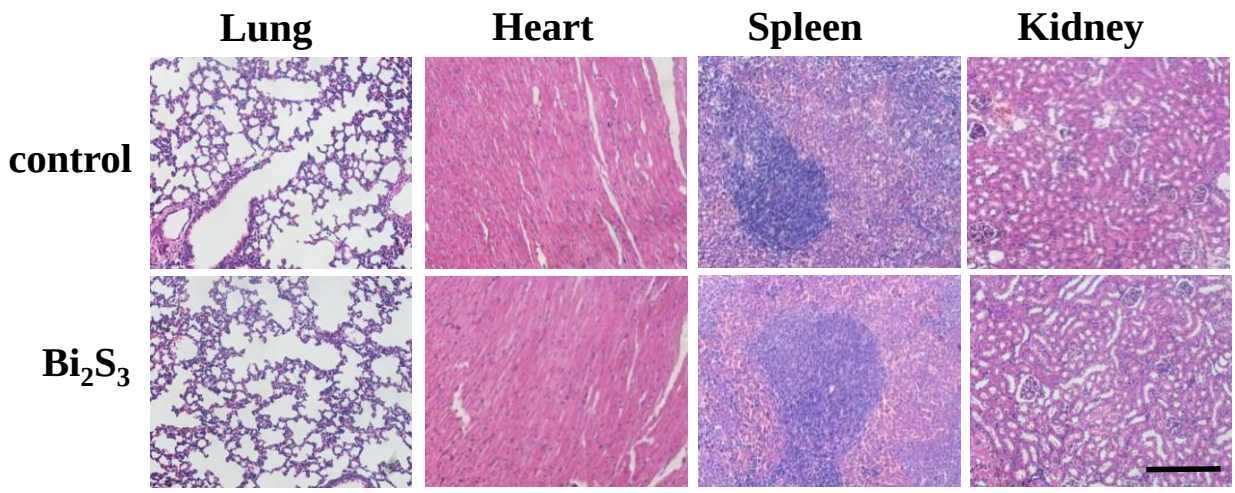

Figure S15. H&E-stained tissue sections from mice to monitor the histological changes in lung, heart, spleen, kidney of mice receiving single intravenous injection of saline (control) or of Bi_2S_3 nanorods followed by dissections in 30 days post-injection. Scale bar corresponds to 100 μm.